Supporting Information

Sothiselvam et al. 10.1073/pnas.1403586111

SI Experimental Procedures

Cell-Free Translation and Toeprinting. Linear DNA templates (0.5–1 pmol) encoding the ORF of interest preceded by the T7 promoter were generated by PCR using primers shown in Table S2. The templates were used to direct transcription–translation in the Δribosome PURExpress cell-free system (New England Biolabs). The reactions were supplemented with antibiotics and with wild-type or mutant ribosomes prepared as described in refs. 1–3 in a total volume of 5 μL. The reactions were incubated for 10 min at 37 °C followed by a 5-min primer extension initiated by addition of reverse transcriptase. cDNA products were separated in a 6% sequencing gel and visualized with a Typhoon imager (GE).

Chemical probing of rRNA was performed using ribosomes prepared according to ref. 3. The 50-μL reactions containing 80 mM K-Hepes, 10 mM $MgCl_2$, 100 mM NH_4Cl and 200 nM ribosomes were preincubated for 5 min at 42 °C. After addition of antibiotic to a final concentration of 50 μM, reactions were incubated for 10 min at 37 °C and 10 min at room temperature. 1-Methyl-7-nitroisatoic anhydride reagent (1M7) (4) was added to a final concentration of 16 mM; after incubation for 1.25 min at 37 °C and 1 min at room temperature, reactions were quenched by addition of stop buffer containing 3 M NaOAc and 0.5 M K-borate. As described previously (5), 1M7-modified RNA was extracted and analyzed by primer extension.

Molecular Dynamics Simulations. All simulations were performed using NAMD 2.9 (6) with the AMBER99SB force field (7, 8), which includes parameters for modified nucleosides (9). Modeling and analysis also used the program VMD (10). The equations of motion were integrated with a 1-fs time step and bonded interactions, nonbonded short-range interactions, and nonbonded long-range interactions were calculated every one, two, and four time steps, respectively. The particle mesh Ewald method (11, 12) was used to evaluate the nonbonded long-range electrostatic interactions. All simulations were carried out in the NpT ensemble at $T = 310$ K and $P = 1$ atm with the following protocol: water and ions were first equilibrated for 2 ns with the remainder of the simulation system restrained, after which side chains of proteins and bases of nucleotides were allowed to move for another 5 ns. Finally, all restraints were released for an equilibration of an additional 10 ns. After these first 17-ns initial equilibrations, production simulations were performed for each system (Fig. S6*D*). All analyses were carried out using only the production simulation data.

The force-field parameters of erythromycin were optimized in two steps. In the first step, the parameterization of partial charges of atoms followed the standard procedure for AMBER, fitting restricted electrostatic potentials generated from quantum mechanics calculations at the RHF/6–31G* level (13). The calculations and fitting were performed using Gaussian (14) and Antechamber (15), respectively. In the second step, all the bonded terms were deduced based on analogous bonded types available in the AMBER99SB force field (7, 8), except for the length of bonds and the values of angles involving heavy atoms, which were taken directly from the crystal structures. The resulting parameter files and the associated topology files needed for simulations with NAMD are available at www.ks.uiuc.edu/~boliu/eryAMBER/.

1. Vazquez-Laslop N, Thum C, Mankin AS (2008) Molecular mechanism of drug-dependent ribosome stalling. *Mol Cell* 30(2):190–202.
2. Vázquez-Laslop N, et al. (2011) Role of antibiotic ligand in nascent peptide-dependent ribosome stalling. *Proc Natl Acad Sci USA* 108(26):10496–10501.
3. Ohashi H, Shimizu Y, Ying BW, Ueda T (2007) Efficient protein selection based on ribosome display system with purified components. *Biochem Biophys Res Commun* 352(1):270–276.
4. Merino EJ, Wilkinson KA, Coughlan JL, Weeks KM (2005) RNA structure analysis at single nucleotide resolution by selective 2′-hydroxyl acylation and primer extension (SHAPE). *J Am Chem Soc* 127(12):4223–4231.
5. Merryman C, Noller HF (1998) Footprinting and modification-interference analysis of binding sites on RNA. *RNA:Protein Interactions, A Practical Approach*, ed Smith CWJ (Oxford Univ Press, Oxford), pp 237–253.
6. Phillips JC, et al. (2005) Scalable molecular dynamics with NAMD. *J Comput Chem* 26(16):1781–1802.
7. Hornak V, et al. (2006) Comparison of multiple Amber force fields and development of improved protein backbone parameters. *Proteins* 65(3):712–725.
8. Cornell WD, et al. (1995) A second generation force field for the simulation of proteins, nucleic acids, and organic molecules. *J Am Chem Soc* 117(19):5179–5197.
9. Aduri R, et al. (2007) AMBER force field parameters for the naturally occurring modified nucleosides in RNA. *J Chem Theory Comput* 3(4):1464–1475.
10. Humphrey W, Dalke A, Schulten K (1996) VMD: Visual molecular dynamics. *J Mol Graphics Modell* 14(1):33–38.
11. Darden Y, York D, Pedersen L (1993) Particle mesh Ewald: An N·log(N) method for Ewald sums in large systems. *J Chem Phys* 98(12):10089–10092.
12. Essmann U, et al. (1995) A smooth particle mesh ewald method. *J Chem Phys* 103(19): 8577–8593.
13. Bayly CI, Cieplak P, Cornell WD, Kollman PA (1993) A well-behaved electrostatic potential based method using charge restraints for deriving atomic charges—the Resp model. *J Phys Chem B* 97(40):10269–10280.
14. Frisch MJT, et al. (2004) Gaussian 03. (Gaussian, Inc., Wallingford, CT), Revision C.02.
15. Wang JM, Wang W, Kollman P, Case DA (2005) Antechamber: An accessory software package for molecular mechanical calculations. *J Comput Chem* 25(9): 1157–1174.

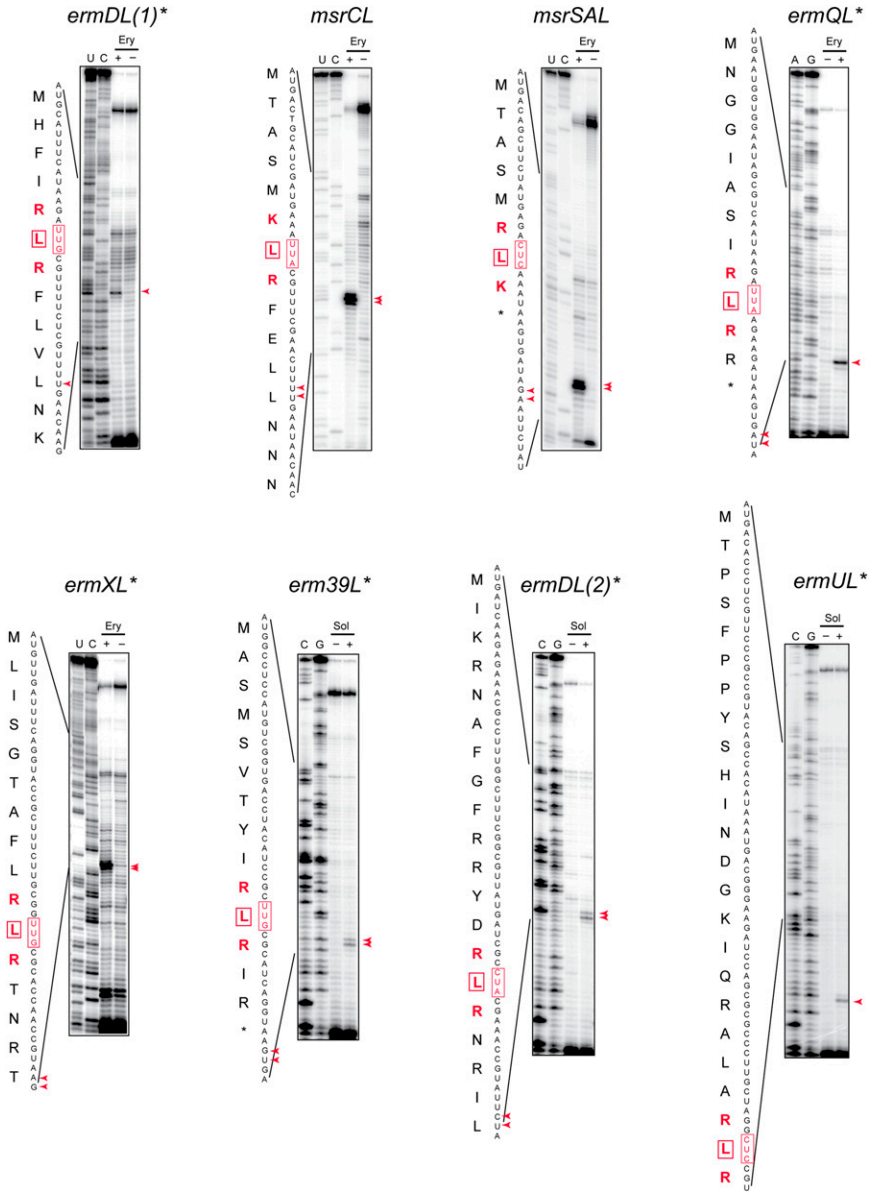

Fig. S1. Antibiotic-dependent ribosome stalling occurs at the R/K-L-R/K motif of leader peptides with heterogeneous N-termini. Erm leader peptides containing the Arg-Leu-Arg (RLR) motif (Table S1) at varying positions were translated in the cell-free system with no antibiotic (–) or with 50 μM of either erythromycin (ERY) or solithromycin (SOL) and analyzed by toe-printing as described in *SI Experimental Procedures*. Arrows indicate the drug-dependent toeprinting signal. The corresponding codon occupying the P site of the stalled ribosome is boxed on the sequences of the leader ORFs shown on the left of each gel.

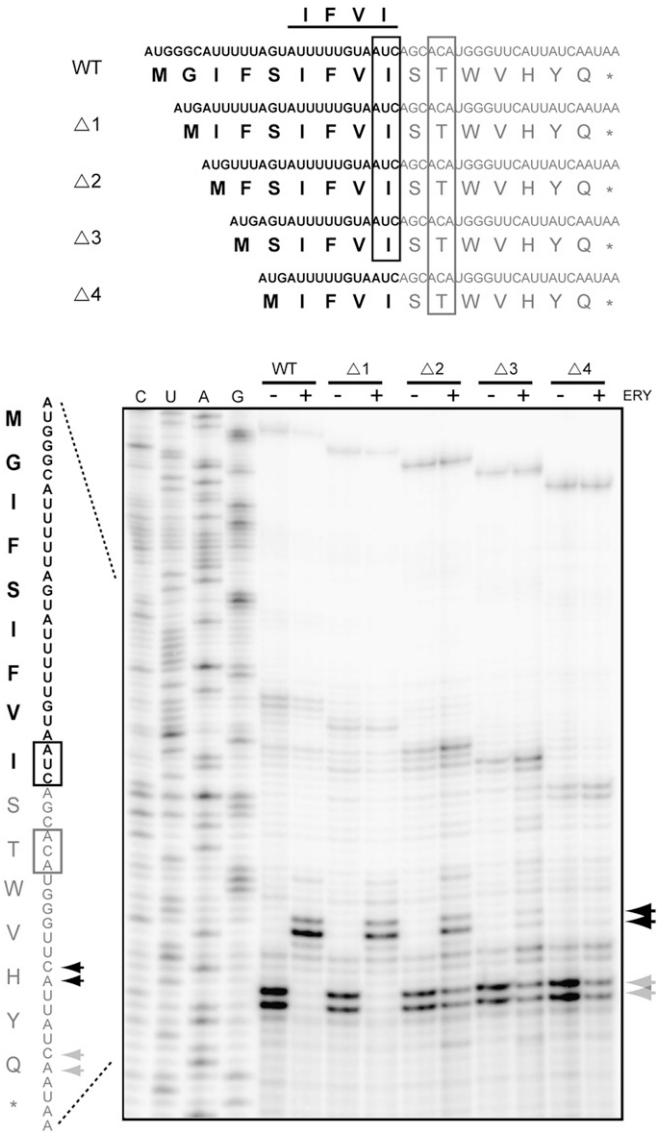

Fig. S2. Drug-dependent ribosome stalling is abolished by the N-terminal truncations of ErmCL. The codons preceding the Ile-Phe-Val-Ile (IFVI) stalling domain of *ermCL* were deleted sequentially to generate truncations Δ1–Δ4. Toeprinting analysis shows reduced ERY-dependent ribosome stalling at the last Ile codon of the IFVI domain (black arrowheads and box). Gray arrows and box show the ERY-independent ribosome capture at the downstream Thr codon due to the lack of Trp–$tRNA^{Trp}$ in the translation reactions depleted by addition of the TrpRS inhibitor indolmycin.

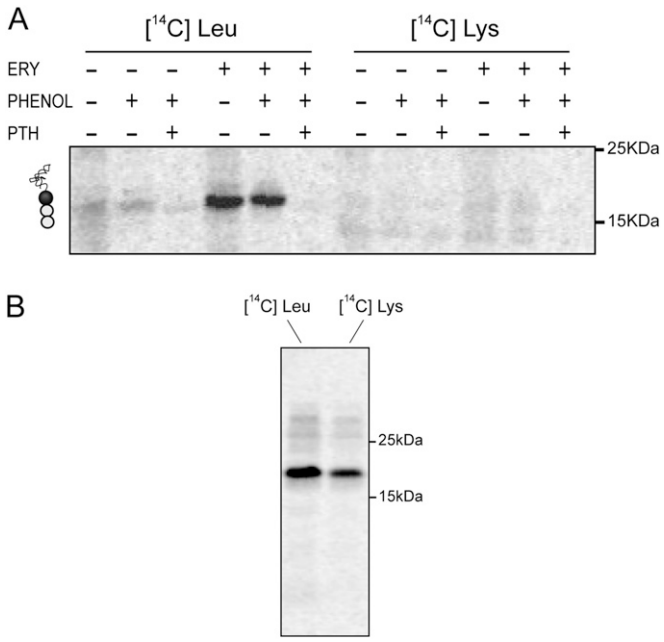

Fig. S3. Characterization of peptidyl–tRNA in the stalled complex. (*A*) Electrophoresis analysis in the Bis-Tris gel system of the [^{14}C]-radiolabeled peptidyl–tRNA accumulating in the course of cell-free translation of the *s-ermDL*(MRLK) template in the absence or presence of ERY. The product, which incorporates [^{14}C]-Leu but not [^{14}C]-Lys, partitions into aqueous phase upon phenol extraction of the reaction and is sensitive to treatment with peptidyl–tRNA hydrolase (PTH). This confirms the peptidyl–tRNA nature of the product represented by strong bands observed in the [^{14}C]-Leu/ERY sample. (*B*) Translation of the control dihydrofolate reductase protein in the cell-free system in the presence of [^{14}C]-Leu or [^{14}C]-Lys, showing that both radioactive amino acids are incorporated efficiently in the protein product.

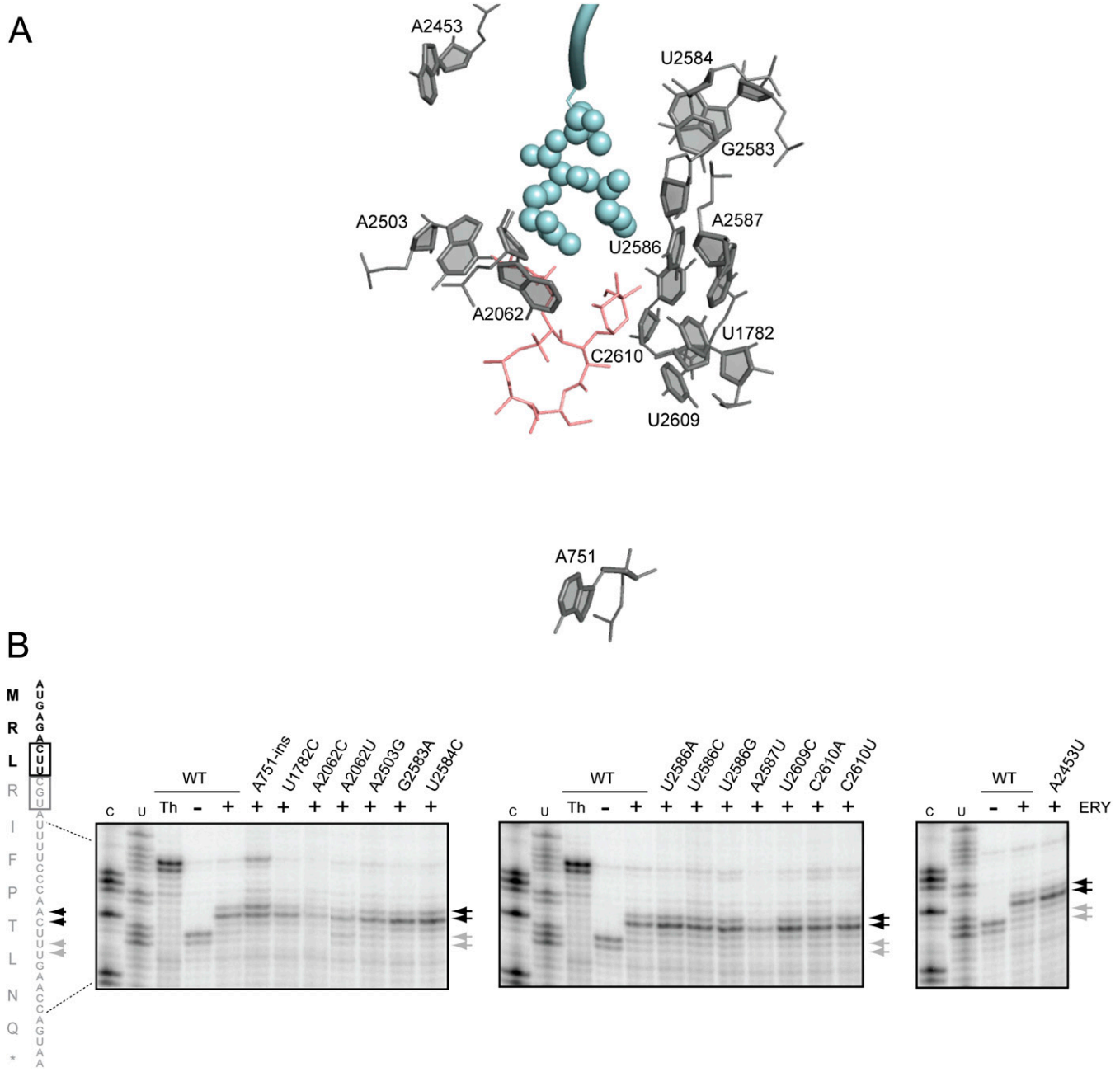

Fig. S4. None of the tested nucleotides in the ribosomal exit tunnel is critical for antibiotic-induced translation arrest with the MRL peptide. (*A*) 23S rRNA residues in the vicinity of the macrolide antibiotic and nascent peptide in the exit tunnel. The MRL peptide was modeled in the structure of the *Escherichia coli* ribosome with bound ERY. The nucleotide residues mutated in this study, which previously were implicated in the mechanism of translation arrest with several stalling peptides, are shown. (*B*) Testing the ability of the mutant ribosomes to form ERY-dependent stalled complex with the MRL peptide. Toeprinting assay was performed in the Δ ribosome PURE cell-free translation system supplemented with wild-type or mutant ribosomes. Black arrows show the ERY-dependent stalling at the Leu codon of the Met-Arg-Leu-Arg (MRLR) sequence of the mutant *s-ermDL* ORF. Gray arrows show the drug-independent capture of the ribosomes at the fourth codon of the ORF due to the presence of the IleRS inhibitor mupirocin in the reactions.

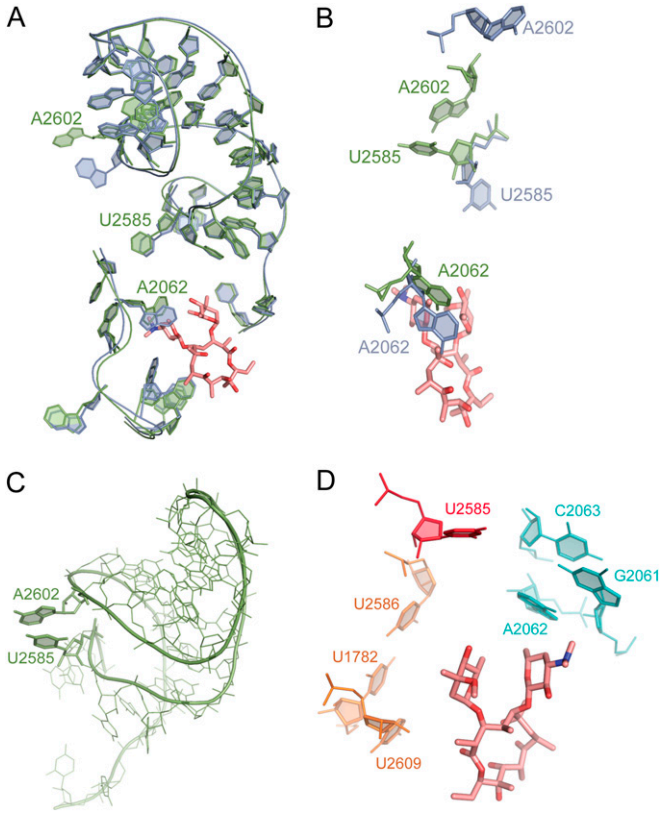

Fig. S5. Molecular dynamics (MD) simulations illuminate the existence of a structural link between the nascent peptide exit tunnel (NPET) and the peptidyl transferase center (PTC). (*A*) The conformation of the NPET and PTC rRNA residues of drug-free (green) and ERY-bound (blue) ribosomes are similar after the initial preproduction equilibration. (*B*) During production simulations, the ERY-proximal A2062 in the NPET and distant U2585 and A2602 in the PTC tend to adopt different conformations. The figure shows the "last-frame" position of the nucleotides averaged over three independent simulations. Green, drug-free ribosome; blue, ERY-bound ribosome. (*C*) The looped-out conformation of U2585 and A2602 in the drug-free ribosome sometimes can be stabilized by possible stacking interactions between the two residues. (*D*) Possible conformational relay routes connecting the macrolide molecule in the NPET to the PTC. The pathway initiated at A2062 is shown in cyan, and the one starting at U2609 is orange. U2585 in the PTC active site is red. The mutations of A2062, U2609, U2586, or U1782 do not abrogate translation arrest controlled by antibiotic and the MRL peptide.

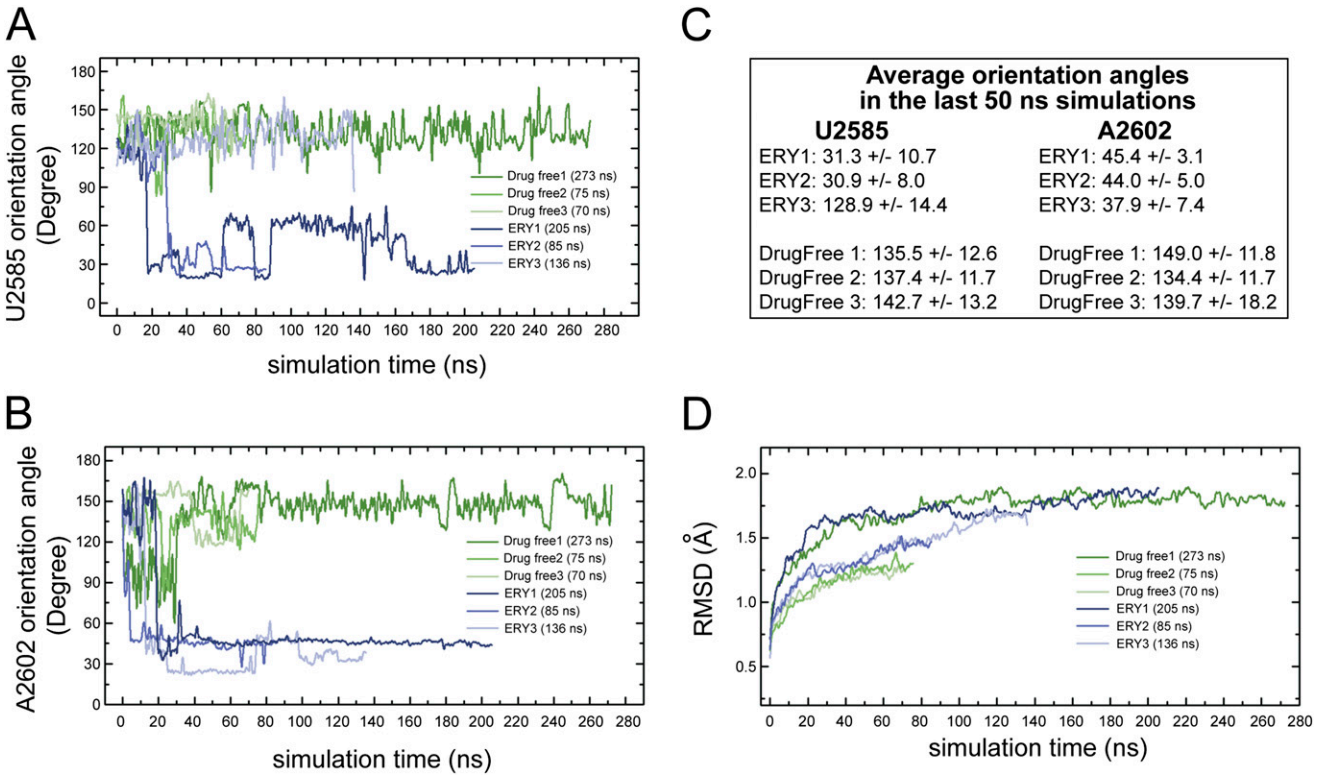

Fig. S6. Equilibration of the ribosome structure and conformations of U2585 and A2602 rRNA residues during MD simulations. (*A*) The changes in the orientation angle of U2585 over simulation time. The orientation angle is defined as in Fig. 6*B*. ERY1, ERY2, and ERY3 are independent simulations of the ERY-bound ribosome. Drug free1, Drug free2, and Drug free3 are independent simulations of the drug-free ribosome. (*B*) Same as *A*, but for A2602. (*C*) Average orientation angles of U2585 and A2602 during the last 50-ns simulations (± SD). (*D*) The rmsd-vs.-time plot for nonhydrogen atoms shows the progress of reaching stable equilibrium during the all-atom ribosome MD simulations. Drug-free and ERY-bound ribosome structures were aligned to reference crystallographic structures 2AVY/2AW4 and 3OFO/3OFR, respectively, and rmsd values were calculated between simulation frames and the corresponding reference structures [2AVY/2AW4 (1) for the drug-free ribosome and 3OFO/3OFR (2) for the ERY-bound ribosome]. All nonhydrogen atoms within 40 Å of U2585 in each system were considered in the rmsd calculations.

1. Schuwirth BS, et al. (2005) Structures of the bacterial ribosome at 3.5 Å resolution. *Science* 310(5749):827–834.
2. Dunkle JA, Xiong L, Mankin AS, Cate JH (2010) Structures of the *Escherichia coli* ribosome with antibiotics bound near the peptidyl transferase center explain spectra of drug action. *Proc Natl Acad Sci USA* 107(40):17152–17157.

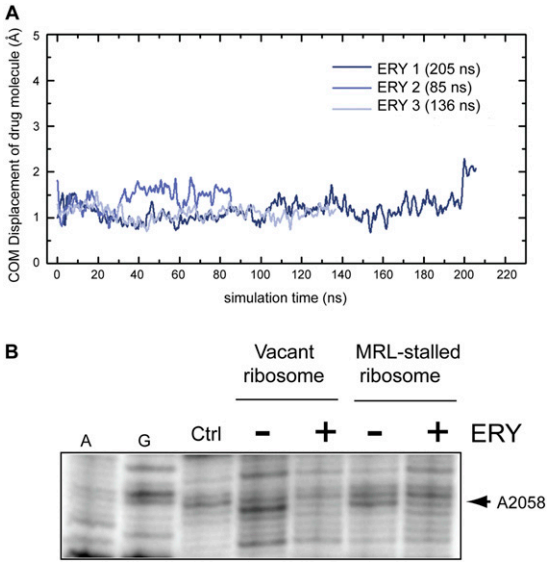

Fig. S7. ERY is stably bound in the tunnel. (*A*) Center-of-mass (COM) displacement plots for the ERY molecule in the tRNA-free ribosome during three independent simulation runs show no tendency for the antibiotic to relocate from its tunnel site. The COM displacement is measured between the COM of ERY in MD simulations and its COM in the crystallographic structure with the Protein Data Bank ID code 3OFR. (*B*) Selective 2′-hydroxyl acylation analyzed by primer extension (SHAPE) probing of the accessibility of A2058 in the ERY binding site in the vacant ribosome or in the ribosome that has synthesized the MRL tripeptide in the cell-free translation system. Note that A2058, which is modified readily by the 1M7 reagent in the absence of ERY, is similarly protected by the antibiotic in the vacant or in the MRL-stalled ribosome.

Table S1. Putative RLR leader peptides of the macrolide resistance genes

Gene[†]	Species	Putative leader peptide[‡]	GenBank PID	GenBank GID	SD score[§]
erm37	*Kribbella flavida*	MGRLRP(28AA)	284033869	284027999	5
*ermZ**	*Streptomyces caelestis*[¶]	MGPRLRR(8AA)	284518868	284518867	4
ermB	*Lactobacillus crispatus*	MEIRLRS(18AA)	33243437	33243436	5
*ermT**	*Lactobacillus fermentum*	MEIRLRS(18AA)	28373207	28373195	5
ermB	*Lactobacillus reuteri*	MEIRLRS(18AA)	2623780	2623778	5
ermB	*Streptococcus pneumoniae*[¶]	MEIRLRS(18AA)	182684297	182682970	5
ermB	*Enterococcus faecium*[¶]	MEIRLRS(18AA)	32470479	32470458	5
ermB	*Lactococcus garvieae*	MEIRLRS(18AA)	187729640	187729634	5
ermB	*Enterococcus faecalis*[¶]	MEIRLRS(18AA)	256965588	242362021	5
ermB	*E. faecalis*[¶]	MEIRLRS(18AA)	305678698	305678685	5
ermB	*Pediococcus acidilactici*	MEIRLRS(18AA)	190410490	190410480	5
ermB	*S. pneumoniae*[¶]	MEIRLRS(18AA)	138752661	138752654	5
*ermD**	*Bacillus clausii*[¶]	MYFIRLRF(5AA)	56965270	56961782	6
*ermD**	*B. clausii*[¶]	MHFIRLRF(5AA)	37359459	37359457	6
ermG	*Bacteroides coprophilus*	MYWTRIRY(16AA)	224026271	221217255	5
ermD	*Bacillus licheniformis*	MTHSMRLRF(6AA)	143201	511060863	6,6
ermJ	*Bacillus anthracis*	MTHSMRLRF(6AA)	730032	143196	6,6
msrSA	*Staphylococcus aureus*[¶]	MTASMRLK	6594277	486222549	7
*ermD**	*Desmospora* sp.	MLVYIRLRF(5AA)	333373800	333373795	7,6
*ermZ**	*S. caelestis*[¶]	MTQSTRLRG(82AA)	284518868	284518867	5
*ermD**	*Paenibacillus* sp.[¶]	MRGVCRIRT(28AA)	261405179	261403876	4
*ermD**	*Paenibacillus* sp.[¶]	MRGVRRIRT(28AA)	329930026	329930019	4
ermB	*Streptococcus suis*	MIVDDKIRI(6AA)	223932186	223932093	6
*erm36**	*Alkaliphilus oremlandii*	MGIASIRIRN(4AA)	158321869	158319059	6
ermB	*Enterococcus gallinarum*	MWIWKVKIKY(15AA)	257869905	239633765	5,8
*ermD**	*Paenibacillus* sp.[¶]	MCCIAFIRIR	261405179	261403876	7
*ermU**	*Tsukamurella paurometabola*	MEPHRYLRIRF(5AA)	296138265	296137750	7
*ermU**	*Microlunatus phosphovorus*	MGIFATIERIRG(1AA)	336117971	336115651	6
*erm39**	*Mycobacterium boenickei*	MAAMSVTHLRLRI(1AA)	73486998	73486996	6,5,5
*erm39**	*Mycobacterium neworleansense*	MASMSVTYIRLRI(1AA)	73487011	73487010	5,5,5
*erm39**	*Mycobacterium houstonense*	MASMSVTYIRLRI(1AA)	73487007	73487005	5,7,7
*ermX**	*Arcanobacterium pyogenes*	MLISGTAFLRLRS(2AA)	38261101	38261095	6
*ermX**	*Corynebacterium glucuronolyticum*	MLISGTAFLRLRT(2AA)	227487333	209951644	6
*ermX**	*Actinomyces* sp.	MLVLGTASLRLRT(1AA)	329944089	329944073	5
ermB	*E. faecium*[¶]	MVNPKVMEIRLRS(18AA)	294617740	294617735	6,5
ermB	*Lactobacillus acidophilus*	MVNPKVMEIRLRS(18AA)	325955700	325955697	6,5
ermB	*Lactobacillus plantarum*	MVNPKVMEIRLRS(18AA)	228860921	228860919	6,5
ermB	*Streptococcus pyogenes*[¶]	MVNPKVMEIRLRS(18AA)	63022016	63021982	6,5
*ermS**	*Streptomyces violaceusniger*[¶]	MPGWRVRASRLRL(20AA)	307329006	307328957	3,6
*erm39**	*Mycobacterium porcinum*	MTAMSVTYLRLRT(1AA)	90901924	90901922	4,4,4
ermQ	*Clostridium bartlettii*[¶]	MIMNGGIASIRLRR	164687690	163813840	8,8
*erm39**	*Mycobacterium wolinskyi*	MAAMSAATFFIRIRI(3AA)	73487015	73487013	4,5
ermB	*Streptococcus agalactiae*	MAEIVKEVMEIRLRS(18AA)	392560	392558	5,5
*ermU**	*Streptomyces* sp.	MGATFAAYALIRLRN(1AA)	302527546	224581096	5
*erm39**	*Mycobacterium mageritense*[¶]	MTDVHNGSPTGRLRS(22AA)	45758647	45758644	5
*erm39**	*M. mageritense*[¶]	MVAMSAACFFIRIRI(1AA)	45758647	45758644	6,6,8
*ermX**	*Kytococcus sedentarius*[¶]	MITAGRLFQRARLRH(14AA)	256825598	256823905	7
*ermD**	*Bacillus halodurans*	MIKRNAFGFRRYDRLRN(16AA)	15612943	57596592	5
*ermX**	*Bifidobacterium thermophilum*[¶]	MDIIRPMLISGTAFLRLRT(2AA)	188593347	188593344	4,7
*ermX**	*B. thermophilum*[¶]	MDIIRPMLISGTAFLRLRT(2AA)	188593350	188593348	4,7
*ermX**	*Corynebacterium diphtheriae*	MDIIRPMLISGTAFLRLRT(2AA)	32470494	32470491	4,7
*ermX**	*Corynebacterium jeikeium*	MDIIRPMLISGTAFLRLRT(2AA)	13517628	13517627	4,7
*ermX**	*Corynebacterium striatum*	MDIIRPMLISGTAFLRLRT(2AA)	32479370	32479367	4,7
ermQ	*C. bartlettii*[¶]	MKGVVVMKNLYIMLNKLKK(10AA)	164687690	163813840	5,8,5
msrC	*E. faecium*[¶]	MCGNLIKKEVGKMTASMKLRF(6AA)	10442770	552941973	4,8,7
*erm36**	*Gordonia bronchialis*	MGTLYSAPSSARNTNMGRLRR(1AA)	262203305	262200046	4,5
*ermU**	*Pseudonocardia* sp.	MRGRHGPANVRAVAAFMRLRV(1AA)	324998303	324330628	6,5,5
ermA	*S. pyogenes*[¶]	MYMYCSSRYYFISFIMKKIKG(22AA)	338795795	338795780	9,7,6
ermA	*S. pyogenes*[¶]	MYMYCSSRYYFISFIMKKIKG(22AA)	94995100	94993396	9,7,6
*ermX**	*K. sedentarius*[¶]	MAVGSPTLVGMLVYGTASLRLRS(1AA)	256825598	256823905	6,6,6
*ermD**	*B. clausii*[¶]	MKCASGVFLFSFTLSRRRFRLRL(4AA)	56965270	56961782	5
*ermZ**	*S. caelestis*[¶]	MRQQAPSNGSSSCRTPADERIRL(49AA)	284518868	284518867	5
erm[‖]	*Nocardia farcinica*	MSRMCAAVNGACAVGAYFIRLRR(15AA)	54024690	54021964	4,6,6,6
*ermD**	*Geobacillus* sp.	MIMLYYYRFLKMEGFLVTFIRLRS(5AA)	312109334	312109151	nd, 7,4,8

Table S1. Cont.

Gene[†]	Species	Putative leader peptide[‡]	GenBank PID	GenBank GID	SD score[§]
ermF	*Bacteroides fragilis*	MLPVICGGYLLFVCIGLGLPRLRI(14AA)	255012163	222299655	6,6,7
*ermS**	*S. violaceusniger*[¶]	MEKGVATGRTRSLRCGDTAEIRIRD(70AA)	307329006	307328957	7
*ermD**	*Paenibacillus* sp.[¶]	MLFYPFHLREDCPDMCCIAFIRIR	329930026	329930019	6,6
*ermU**	*Catenulispora acidiphila*	MTPSFPPYSHINDGKIQRALARLRD(17AA)	256395256	256389232	8
ermB	*S. aureus*[¶]	MGEKWPSRVLGTFNSSVPTRVVKLRS	329315326	329312723	4,4
ermB	*S. pneumoniae*[¶]	MYFSICNRRVLFTKLLAGRGPERLRG(6AA)	182683142	182682970	nd, 5
*ermE**	*Thermomonospora curvata*	MHTCAAPPGGAAAPAACAPAFRRLRT(9AA)	269124773	269124277	5
*erm39**	*Mycobacterium fortuitum*	MGQAHRRSRAEIELSVRPRAPTVAAMSVTYIRLRI(1AA)	40807669	40807664	5,5,5,5

Methyltransferase proteins of the Erm class were searched in the National Center for Biotechnology Information "nr" database with PSI-BLAST using *Streptomyces venezuelae* PikR1 (GenInfo Identifier number 3800833) as the query. The sequences were aligned with MAFFT (1), and after ambiguously aligned regions were removed, phylogenetic analysis was carried out with RaxML (2) to classify the sequences into the various subgroups of Erm methyltransferases. The reconstructed phylogenetic tree is available upon request from G.C.A. (gemma.atkinson@gmail.com) or T.T. (tanel.tenson@ut.ee). Search for upstream ORFs were performed within 500 bps upstream from the start of Erm-like methyltransferase genes. Several macrolide efflux pump genes known to be controlled by the leader ORFs were added to the table. The upstream sequences were translated in all three reading frames and scanned for ORFs starting with AUG or GUG codons and containing at least five codons. The ORFs encoding peptides containing the (R/K)(L/I)(R/K) motifs were selected, and the putative Shine–Dalgarno sequences within 21 bp upstream from a possible start codon were identified.

[†]The names of the *erm* genes previously assigned to a specific *erm* class are shown without asterisks. Genes whose class assignment is based on the proximity in the phylogenetic tree are indicated by asterisks. Leader ORFs at which ribosome stalling was assessed experimentally (Fig. S1) are highlighted in yellow. The *ermDL* ORF, which was subjected to truncation mutagenesis and detailed biochemical analysis, is highlighted in cyan.

[‡]The peptides with the initiator site within 25 codons upstream from the conserved motif are shown. Alternative potential initiation sites (corresponding to in-frame AUG or GUG codons) are indicated by boldface characters.

[§]The Shine–Dalgarno score (SD score) was computed by calculating the number of identical nucleotides of the best match within 21 bp upstream from a possible start codon to the idealized sequence AAGGAGGTGATC. When the first initiator codon was within less than 12 nt from the beginning of the available sequence, SD score was not determined (nd).

[¶]Same species, different strains.

[‖]No single closely homologous *erm* gene.

1. Katoh K, Kuma K, Toh H, Miyata T (2005) MAFFT version 5: Improvement in accuracy of multiple sequence alignment. *Nucleic Acids Res* 33(2):511–518.
2. Stamatakis A (2006) RAxML-VI-HPC: Maximum likelihood-based phylogenetic analyses with thousands of taxa and mixed models. *Bioinformatics* 22(21):2688–2690.

Table S2. Primers used in the study

Name	Sequence
T7	TAATACGACTCACTATAGGG
NV1	GGTTATAATGAATTTTGCTTATTAAC
ERMD-I-F	TATACGACTCACTATAGGGCTTAAGTATAAGGAGGAAAAAATATGACACACTCAATGAGACTTCGTTTCCCAATTACTTTGAACCAG
S6DL-I-F	TAATACGACTCACTATAGGGCTTAAGTATAAGGAGGAAAAAATATGCACTCAATGAGACTTCGTTTCCCAATTACTTTGAACCAG
S5DL-I-F	TAATACGACTCACTATAGGGCTTAAGTATAAGGAGGAAAAAATATGTCAATGAGACTTCGTTTCCCAATTACTTTGAACCAG
S4DL-I-F	TAATACGACTCACTATAGGGCTTAAGTATAAGGAGGAAAAAATATGATGAGACTTCGTTTCCCAATTACTTTGAACCAG
S3DL-I-F	TAATACGACTCACTATAGGGCTTAAGTATAAGGAGGAAAAAATATGAGACTTCGTTTCCCAATTACTTTGAACCAGTAAGTGATAG
S2DL-I-F	TAATACGACTCACTATAGGGCTTAAGTATAAGGAGGAAAAAATATGCTTCGTTTCCCAATTACTTTGAACCAG
ERMDL-I-R	GGTTATAATGAATTTTGCTTATTAACGATAGAATTCTATCACTTACTGGTTCAAAGTAATTGGG
MUT-R	GGTTATAATGAATTTTGCTTATTAACGATAGAATTCTATCACTTACTGGTTCAAA
MRLK-I-F	TAATACGACTCACTATAGGGCTTAAGTATAAGGAGGAAAAAATATGAGACTTAAATTCCCAATTACTTTGAACCAGTAAGTGATAG
S3DL-R4K-STOP-FWD	TAATACGACTCACTATAGGGCTTAAGTATAAGGAGGAAAAAATATGAGACTTAAATAAGTGATAGAATTCTATC
S3DL-R4K-STOP-REV	GGTTATAATGAATTTTGCTTATTAACGATAGAATTCTATCACTTA
L2667	GGTCCTCTCGTACTAGGAGCAG
S8CL-W-F	AATACGACTCACTATAGGGCTTAAGTATAAGGAGGAAAAAATATGGGCATTTTTAGTATTTTTGTAATCAGCACATGGGTTCATTAT
S7CL-W-F	TAATACGACTCACTATAGGGCTTAAGTATAAGGAGGAAAAAATATGATTTTTAGTATTTTTGTAATCAGCACATGGGTTCATTAT
S6CL-W-F	TAATACGACTCACTATAGGGCTTAAGTATAAGGAGGAAAAAATATGTTTAGTATTTTTGTAATCAGCACATGGGTTCATTAT
S5CL-W-F	TAATACGACTCACTATAGGGCTTAAGTATAAGGAGGAAAAAATATGAGTATTTTTGTAATCAGCACATGGGTTCATTAT
S4CL-W-F	TAATACGACTCACTATAGGGCTTAAGTATAAGGAGGAAAAAATATGATTTTTGTAATCAGCACATGGGTTCATTAT
ERMCL-R	GGTTATAATGAATTTTGCTTATTAACGATAGAATTCTATCACTTATTGATAATGAACCCATGTGCTGA
MRLR-I-F	TAATACGACTCACTATAGGGCTTAAGTATAAGGAGGAAAAAATATGAGACTTCGTATTTTCCCAACTTTGAACCAG
ERMDL-NEW MUP-R	GGTTATAATGAATTTTGCTTATTAACGATAGAATTCTATCACTTACTGGTTCAAAGTTGGGAA
MSR-C-F	TAATACGACTCACTATAGGGCTTAAGTATAAGGAGGAAAAAATATGAC
	TGCATCGATGAAATTACGTTTCGAACTTTTGAATA
MSR-C-R	GGTTATAATGAATTTTGCTTATTAACGATAGAATTCTATCACTTAGTTGT
	TATTCAAAAGTTCGAAACGTAAT
MSR-SA-F	TAATACGACTCACTATAGGGCTTAAGTATAAGGAGGAAAAAATATGAC
	AGCTTCTATGAGACTCAAATAA
MSR-SA-R	GGTTATAATGAATTTTGCTTATTAACGATAGAATTCTATCACTTATTTGA
	GTCTCATAGAAGCTGTC
ERMDL (1)*-F	TAATACGACTCACTATAGGGCTTAAGTATAAGGAGGAAAAAATATGCA
	TTTCATAAGATTGCGTTTTCTCGTTTTG
ERMDL (1)*-R	GGTTATAATGAATTTTGCTTATTAACGATAGAATTCTATCACTTACTTGT
	TCAAAACGAGAAAACGCAATC
ERM39*-F	TAATACGACTCACTATAGGGCTTAAGTATAAGGAGGAAAAAATATGGCCTCCATGTCGGTGACCTACATCCGCTTGCGCATCAGGTAA
ERM39*-R	GGTTATAATGAATTTTGCTTATTAACGATAGAATTCTATCACTTACCTGATGCGCAAGC
ERMDL (2)*-F	TAATACGACTCACTATAGGGCTTAAGTATAAGGAGGAAAAAATATGATCAAGAGAAACGCCTTTGGCTTTCGGCGTTATGATCGCCTACG
ERMDL (2)*-R	GGTTATAATGAATTTTGCTTATTAACGATAGAATTCTATCACTTATAATAGAATACGGTTTCGTAGGCGATCATAACGCC
ERMUL-F	TAATACGACTCACTATAGGGCTTAAGTATAAGGAGGAAAAAATATGACACCCTCGTTCCCGCCGTACAGCCACATAAATGACGGGAAGAT
ERMUL-R	GGTTATAATGAATTTTGCTTATTAACGATAGAATTCTATCACTTAACGGAGCCTAGCAAGGGCGCGCTGGATCTTCCCGTCATTTATGT
ERMXL*-F	TAATACGACTCACTATAGGGCTTAAGTATAAGGAGGAAAAAATATGTT
	GATTTCAGGTACCGCTTTCTTGCGGTTGCGCAC
ERMXL*-R	GGTTATAATGAATTTTGCTTATTAACGATAGAATTCTATCACCTACGGG
	GTAGGAAACGCCTTACGGTTGGTGCGCAACCGCAAGAAAG
ERMQL*-F	TAATACGACTCACTATAGGGCTTAAGTATAAGGAGGAAAAAATATGAATGGTGGAATAGCGTCAATAAGATTAAGAAGAT
ERMQL*-R	GGTTATAATGAATTTTGCTTATTAACGATAGAATTCTATCACCTATCTTCTTAATCTTATTGAC

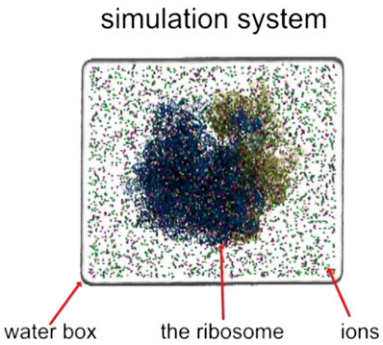

Movie S1. Conformational rearrangement of the PTC residues U2585 and A2602 induced by binding of ERY in the ribosomal exit tunnel; MD simulations.

Movie S1